Supplementary Information

Release of microplastics and metals from antifouling paint during weathering

Guadalupe Santos[1], Georgina C. Kalogerakis[1], Jun-Ray Macairan[1], Laura M. Hernandez[1], Houssame-Eddine Ahabchane[2], Jennifer F. Provencher[3], Kevin J. Wilkinson[2*] and Nathalie Tufenkji[1, 4*]

[1]Department of Chemical Engineering, McGill University, Montreal, Quebec, H3A 0C5 Canada
[2]Department of Chemistry, University of Montréal, Montreal, Quebec, H2V 0B33, Canada
[3]Environment and Climate Change Canada, National Wildlife Research Centre, Ottawa, Ontario, K1A 0H3, Canada
[4]United Nations University Institute for Water, Environment and Health, Richmond Hill, Ontario, L4B 3P4, Canada

[*] Corresponding author: nathalie.tufenkji@mcgill.ca, kj.wilkinson@umontreal.ca

Number of Figures: 12
Number of Tables: 6
Number of Text:1
Number of Pages: 25

Table S1. Summary of literature examining the release of nanoplastics, microplastics, and metals from various types of paints.

Category of paint products released		Paint type	Sizes observed (average or range)	Concentration range or percentage composition released	Main analytical techniques*	Weathering conditions	Ref.
nanoplastics	polyacrylate	building paints	97 – 98 nm	not specified	SEM-EDX, Raman, DLS, FTIR, AF-FFF	laboratory: dispersed in demineralized water	Müller *et al.*, 2022a[1]
	suspected styrene or acrylic	building paints	<500 nm	not specified	SEM-EDX, Raman	none	Fang *et al.*, 2024[2]
microplastics	unidentified thermoplastic	road marking paints	1 – 4 mm	18.5 ± 4.2 – 66 ± 7.7 particles/100 g of river water	optical microscopy, Raman	natural: river	Horton *et al.*, 2017[3]
	alkyds poly(acrylate/ styrene)	Industrial paints, marine based paints	<50 – 500 µm	171 ± 113 particles/L 24 ± 21 particles/L	FTIR	natural: seacoast in Korea	Song *et al.*, 2014[4]
	polyurethane	contamination from the research vessel, marine based paints	0.3 – 23 mm	2805 particles/ 9127 m^3 filtered seawater	FTIR, SEM	natural: Antarctic peninsula	Lacerda *et al.*, 2019[5]
	not specified	marine based paints	0.1 – 5 mm	maximum approximately 900 particles/m^2	optical microscopy	natural: coastal sediments in Campeche Bay, Mexico	Borges Ramirez *et al.*, 2019[6]
	alkyd, epoxy, chlorinated rubber	marine based paints, building paints and road marking paints	180 µm (median)	0.01 paint particles/m^3	XRF, ATR-FTIR	natural: North Atlantic Ocean	Turner *et al.*, 2022[7]
	not specified	marine based paints	1 – 3 mm	12.8% out of 398 microplastic particles	optical microscopy	natural: sediments from the Paranaguá Estuarine Complex	Mengatto & Nagai, 2022[8]
	acrylates polyurethane varnish (APV)	marine based paints	<75 µm	mean numerical proportion: 70 ± 19%	µFTIR, ATR-FTIR, optical	natural: Sediments from Rhine River	Mani *et al.*, 2019[9]

					microscopy		
	thermosetting polyester, epoxy resins	marine based paints	not specified	not specified	FTIR	natural: coastal waters of plymouth	Higgins & Turner, 2023[10]
	alkyd resin, poly(acrylate/ styrene)	marine based paints	50 – >1000 µm	98.7% in surface microlayer 99.6% in surface seawater-hand net 60% in surface seawater -trawl net	FTIR	natural: surface sea waters of Korean west coast	Chae *et al*., 2015[11]
	not specified	marine based paints	0.3 – 5 mm	0.03 – 0.65 paint particles/m^3	FTIR, optical microscopy	natural: surface waters of Korea	Kwon *et al*., 2020[12]
	not specified	marine based paints	1 – 5 mm >5 mm	80% of total mesoparticles 32% of total macroplastics	ATR-FTIR, SEM-EDX	natural: sediments in Tunisian coast	Jaouani *et al*., 2022[13]
	not specified	marine based paints	<0.4 mm (mean)	12% of total plastic particles	optical microscopy	natural: plankton samples in Western Tropical Atlantic Ocean	Ivar do Sul *et al*., 2014[14]
	alkyd	marine based paints, contamination from the research vessel	<2 mm	0.94 to 232 particles/m^3	optical microscopy, FTIR	natural: southeastern coast of Korea	Kang *et al*., 2015(Kang et al., 2015)
	not specified	marine based paints	<5 mm	29% of total particles	optical microscopy	natural: plankton samples in Western Tropical Atlantic Ocean	Lima *et al*., 2014[16]
	not specified	marine based paints	4 µm – <10 mm	58 ± 58 particles/m^2	Raman	natural: sediments from Lake Garda	Imhof *et al*., 2016[17]
	not assignable but suspected APV polyester oxide	marine based paints, contamination from the research vessel	101 – 8932 µm	48% of total plastic particles	µXRF, ATR-FTIR	natural: surface and subsurface water samples from Weddell Sea	Leistenschneider *et al*., 2021[18]
	poly(methyl methacrylate) polyvinyl chloride polycarbonate	marine based paints	<1000 µm	Highest values: 53% (PMMA), 38% (PVC), 2% (PC)	py-GC-MS	natural: the German Bight (North Sea)	Dibke *et al*., 2021[19]

	not specified	marine based paints	not specified	0.01 – 3 mm	optical microscopy, Raman, SEM-EDX	natural: marinas on the Swedish coast	Gondiaks *et al*., 2023[20]
Metal nanoparticles	TiO_2 Ag SiO_2	industrial paint	TiO_2: <10 nm Ag: 40 and 90 nm SiO_2: 12 nm	TiO_2: 4–8 µg/L Ag: Under detection limit (0.1 µg/L) SiO_2: 73 mg/L (1.8% of total SiO_2 in paint)	ICP-OES, TEM-EDX, XRF	laboratory: UV irradiation (500 h, UV-A), abrasion (500 g load with 500 cycles/rotation)	Zuin *et al*., 2014[21]
	SiO_2	industrial paint	12 nm	0.065 mg/L (2.3% of the total nano-SiO_2 in panels)	ICP-OES, TEM-EDX	laboratory: UV irradiation and precipitation (89 six-hour cycle, UV-A)	Al-Kattan *et al*., 2015[22]
	TiO_2 Ag SiO_2	industrial paint	Ti: 30 nm Ag: 50 nm Si: 10 nm	Ti: 0.00048‰ Ag: 0.025‰ to 0.055‰ Si: 0.38–0.62%	ICP-MS, DLS	laboratory: static water immersion test, UV irradiation (UV-A, 63 cycles of 8 h each), precipitation (500 h)	Zhang *et al*., 2017[23]
	TiO_2	building paint	20 – 60 nm	<0.001% of total nano-TiO_2 in paint	SP-ICP-MS	natural: 10 weeks winter, 7 weeks summer laboratory: Room temperature, freezing (-10 C), freeze thaw (24 h freeze, 24 h thaw) for 42 days	Azimzada *et al*., 2020a[24]
	TiO_2	building paint	20 – 300 nm	maximum 600 µg/L	ICP-MS, ICP-OES, TEM-EDX	natural: runoff (1 rain event)	Kaegi *et al*., 2008[25]
	CeO_2	building paint, stain	17.5 nm (paint), 16.6 nm (stain)	15% (paint) and 35% (stain) of total NP-Ce in paint	SP-ICP-MS	natural weathering: 11 weeks starting Oct and 12 weeks starting Jan	Jreije *et al*., 2022[26]
	Ag	building paint	Ag: <15 nm	30% of total NP-Ag in paint	ICP-MS, TEM-EDX	natural: runoff (65 runoff events, 372 days)	Kaegi *et al*., 2010[27]
	TiO_2	building paint	up to 100 nm (in supernatant)	not applicable	DLS, SEM-EDX, AF-FFF, Raman	laboratory: dispersed in milli-q water	Muller *et al*., 2022a[1]
	Cu_2O	marine based paints	40 – 460 nm	0.21% of total Cu in paint (aluminum bars, 180 days) 1.76% of total Cu in	SP-ICP-MS, DLS, SEM-EDX	laboratory: submerged panels with fluorescent light exposure and shaking (simulates natural waters)	Adeleye *et al*., 2016[28]

				paint (wood bars, 180 days)		for 180 d	
	TiO_2	building paint, stain	20 – > 200 nm	10^{-4}% of total TiO_2 in paint 6% of total TiO_2 in wood stain	SP-ICP-MS, SP-ICP-TOF-MS	natural: 11 weeks starting Oct and 12 weeks starting Jan	Azimzada *et al*., 2020b[29]
	TiO_2	industrial paint	20 – 80 nm	0.007% of total nano-TiO_2	SEM-EDX, TEM	laboratory: 113 cycles, 6 h (3 hours of UV irradiation (UV-B), 0.5 h of irrigation and 2.5 h of drying)	Al-Kattan *et al*., 2013[30]
	Cu	marine based paints	45 – 100 nm	maximum 1.2 x 10^7 particles/m^3	SP-ICP-MS	natural: marinas on the Swedish coast	Gondikas *et al*., 2023[20]
Total metals	Cu Zn	marine based paint	not available	Cu: ~16.0% of total Cu in dry paint (maximum) Zn: ~11.0% of total Zn in dry paint (maximum)	ICP-OES	laboratory: room temperature (19 °C) or in refrigerator (4 °C) for 120 h; different salinities	Singh & Turner, 2009[31]
	Cu Zn	marine based paint	not available	Cu: 70 µg/cm^2 day (acrylic, maximum) Zn: 64 µg/cm^2 day (acrylic, maximum)	AAS	laboratory: submerged in artificial sea water with wave-like conditions and at room temperature (23 °C)	Jalaie *et al*., 2023[32]
	Al S Cu Zn Cd Pb	marine based paint	not available	All percentages are maximums. Zn: 2.0% (paint mix), 0.1% (Alusafe) Cu: 0.2% (paint mix), 0.9% (Alusafe) S: 26.0% (paint mix), 5.0% (Alusafe) Cd: 4.5% (paint mix), 0.7% (Alusafe) Pb: 0.1% (paint mix) Al: 0.7% (Alusafe)	ATR-FTIR, ICP-OES	laboratory: UV irradiation (UV-C) for 21 days, leaching in algae growth media for 168 h	Simon *et al*., 2021[33]
	Cu Zn	marine based paint	not available	Cu: 10.0 – 15.0% loss Zn: <8.0% loss	ICP-OES	laboratory: submerged in artificial sea water, with 12 h light-dark cycles using fluorescent tubes for 80 h	Holmes & Turner, 2009[34]
	Cu Zn	marine based paint	not available	Cu: 0.5% – 3.0% loss in aqueous phase	ICP-OES	laboratory: submerged in tap water (pH 7.3) or rainwater	Jessop & Turner,

				Zn: 5.0 – 30.0% loss in aqueous phase		(pH 4.7) for 120 h	2011[35]

*AAS = atomic absorption spectroscopy; AF-FFF = asymmetric flow-field flow fractionation; FTIR = Fourier transform infrared spectroscopy; ATR-FTIR = attenuated total reflectance FTIR; DLS: dynamic light scattering; EDX = energy-dispersive X-ray spectroscopy; ICP-MS = inductively coupled plasma time-of-flight mass spectrometry; ICP-OES = inductively coupled plasma optical emission spectroscopy; py-GC-MS = pyrolysis gas chromatography-mass spectrometry; SEM = scanning electron microscopy; SP-ICP-TOF-MS = single particle inductively coupled plasma time-of-flight mass spectrometry; TEM = transmission electron microscopy; and XRF = X-ray fluorescence.

Table S2. Composition of MicronCSC-CA antifouling paint[36] and base Interprotect2000E primer paint,[37] according to the manufacturer (Interlux®).

MicronCSC-CA antifouling paint		**base Interprotect2000E primer paint**	
Ingredient	**Weight percentage (%)**	**Ingredient**	**Weight percentage (%)**
copper (I) oxide	30 - 60	polymer of epoxy resin and bisphenol A	10 - 25
zinc oxide	10 - 30	talc	10 - 25
xylene	7 - 13	barium sulfate	10 - 25
iron oxide	3 - 7	titanium dioxide	10 - 25
butyl alcohol, n-	3 - 7	mica	1.0 - 10
ethyl benzene	1 - 5	xylenes	1.0 - 10
ethyl toluene sulfonamide	1 - 5	butanol	1.0 - 10
copper (II) oxide	1 - 5	petroleum naphtha	1.0 - 10
		1,2,4-trimethyl benzene	1.0 - 10
		benzene, ethyl-	1.0 - 10
		1,3,5-trimethylbenzene	1.0 - 10

Figure S1. Spectrum of the UV lamp (Arcadia 54w T5 D3+ 6% UVB 46", ReptilesRuS) as provided by the manufacturer. The x-axis denotes the wavelength (nm); the y-axis denotes the relative intensity of the light.

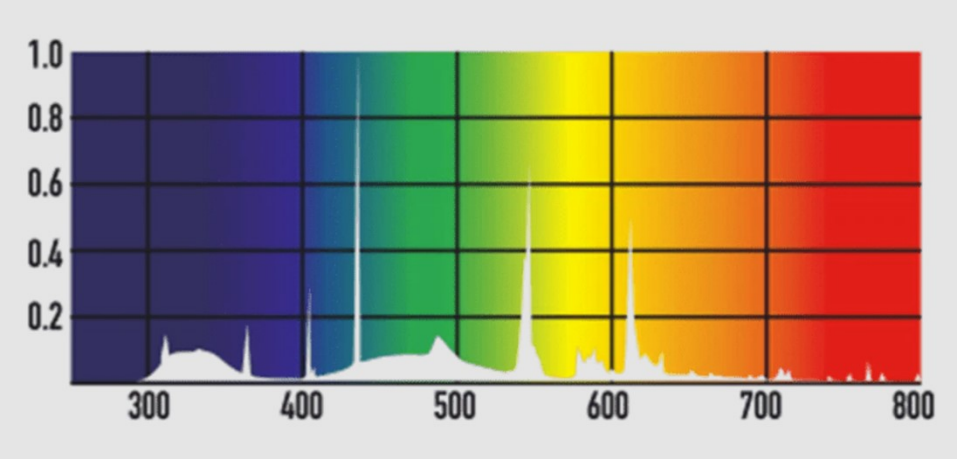

Text S1. The equivalent UV irradiation used in this experiment was calculated using a measured average UV radiation of 12.7 ± 1.0 W m-2 during the 21 days the UV lamps were turned on. Using the yearly radiant exposure data in Canada (49000 W h m^{-2}/year) used by Hernandez et al. (2023), [38] the corresponding real-world UV radiation was calculated as follows:

$$12.7\ W \cdot m^{-2} \times 24\frac{h}{day} = 304.8\ W \cdot h \cdot m^{-2}\ per\ day$$

$$304.8\ W \cdot h \cdot m^{-2}\ per\ day \times 21\ days = 6400\ W \cdot h \cdot m^{-2}$$

$$\frac{6400\ W \cdot h \cdot m^{-2}}{49000\ W \cdot h \cdot \frac{m^{-2}}{year}} = 0.1306\ years = 47.7\ days$$

Figure S2. Nujol mull spectrum of the suspected rosin (CAS 8050-09-7). Major peaks (cm-1) are listed with their corresponding transmittance (%). The spectrum is provided by the Chemical Book.[39]

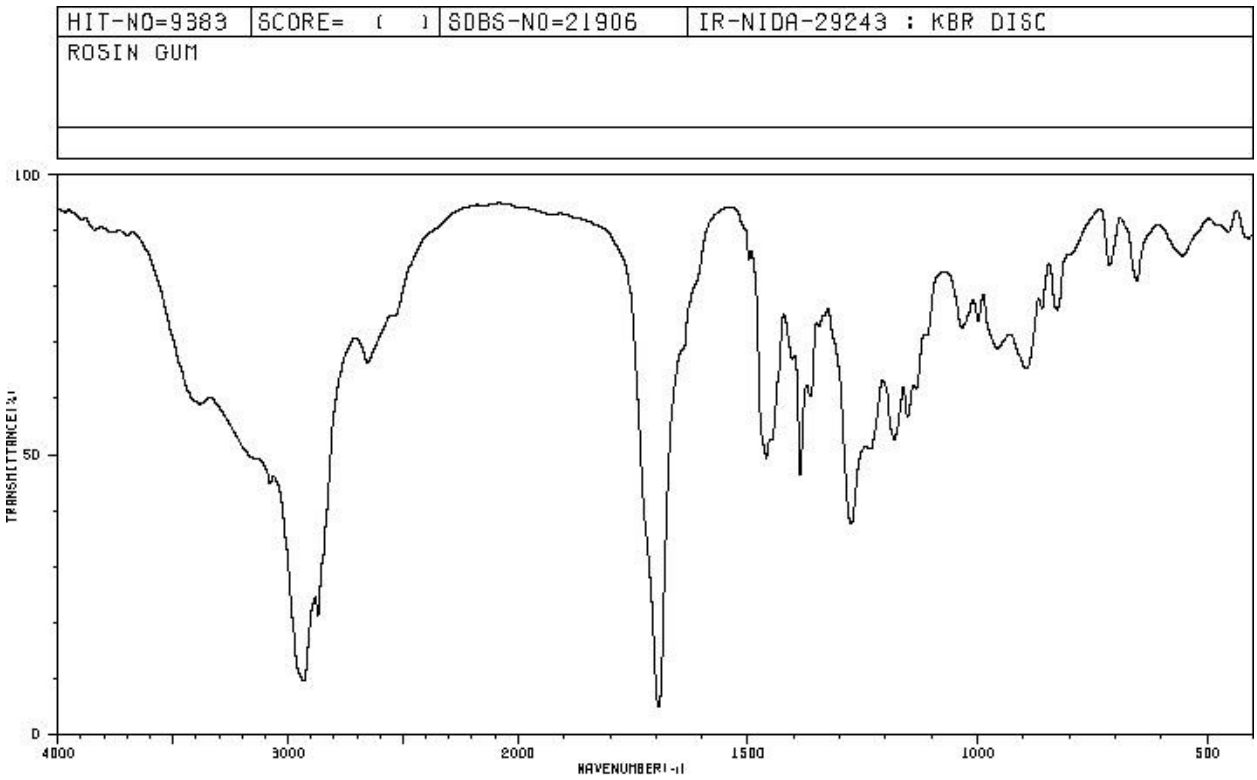

3382	67	1498	81	1189	62	893	62
3078	43	1460	47	1182	50	860	72
2950	10	1449	50	1153	55	828	72
2933	9	1386	44	1033	70	713	81
2869	20	1372	60	998	70	653	79
2853	64	1364	58	956	86	554	81
1694	4	1276	36	901	64	466	86

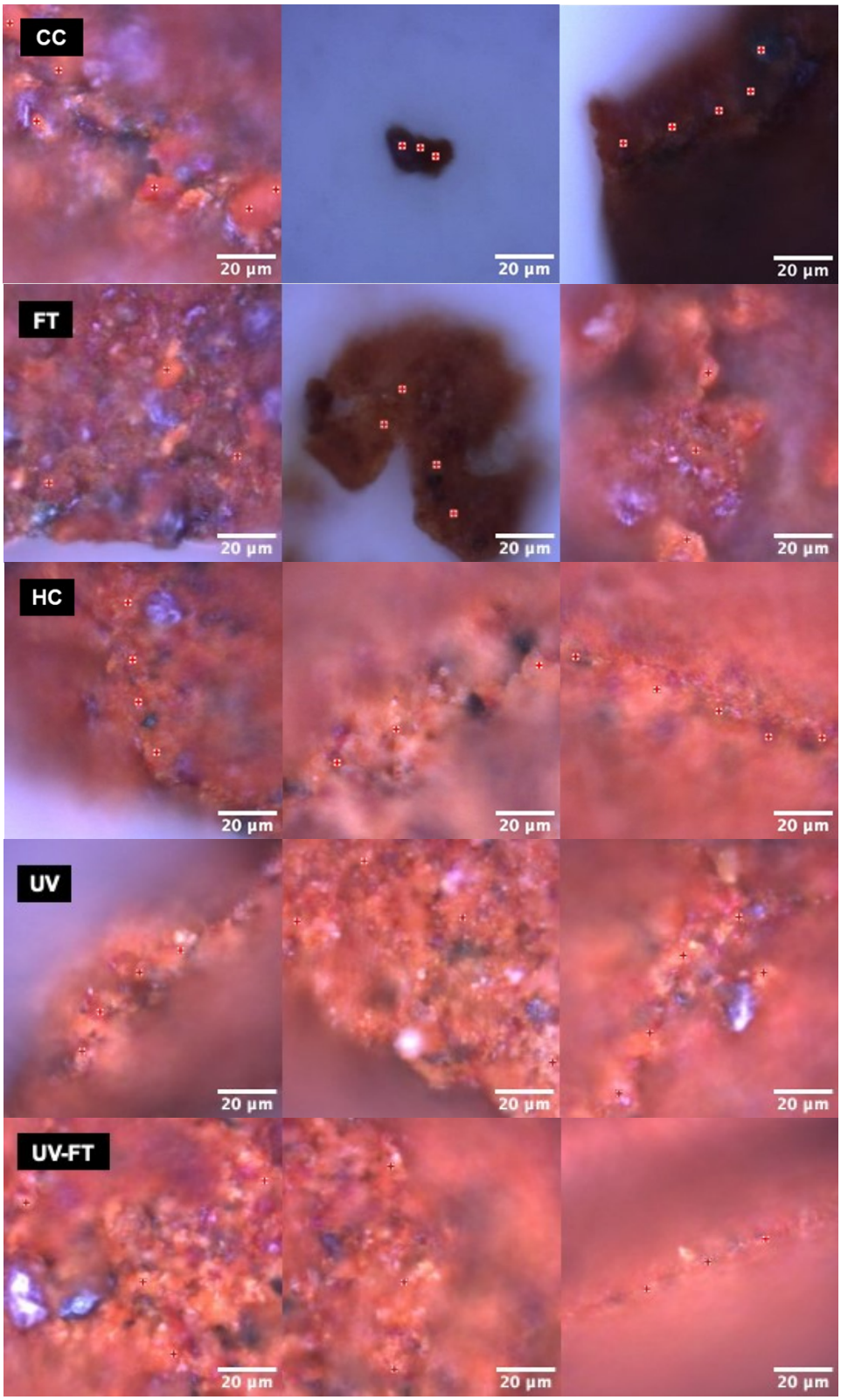

Figure S3. Representative images of antifouling paint microplastics of controls (CC and HC) and weathering treatments (UV, FT, and UV-FT) imaged on the filter, from which the O-PTIR spectra were acquired. Each row corresponds to one weathering condition, and the three columns show

77 replicate particles selected for that condition to demonstrate within-treatment variability. Red
78 markers indicate where OPTIR spectra were acquired and depict the morphology and visual
79 appearance of the analyzed paint fragments for the specific condition.

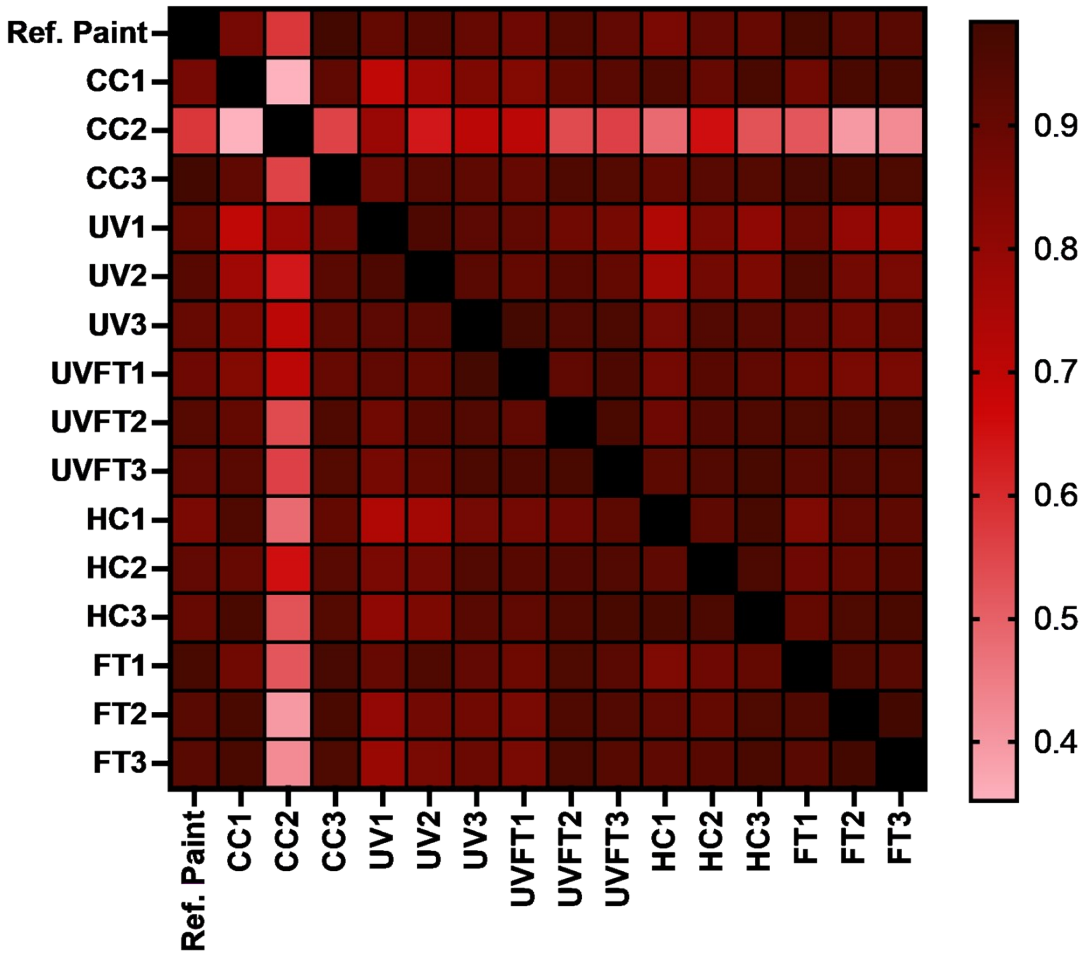

Figure S4. A heatmap of Pearson correlation coefficients comparing weathered antifouling paint microplastics from treatments and reference antifouling paint (denoted as Ref. Paint). Nine spectra were averaged for each comparison. Treatments are denoted as CC = cold control, HC = heat control, UV = UV irradiation, FT = freeze-thaw, and UV-FT = UV and FT combination. Each replicate is denoted after the treatment name (e.g., CC1, CC2, and CC3). Black squares indicate that the correlation is equal to 1.

Text S2. CC had the lowest calculated coefficient yet experienced the least weathering exposure. Replicate 2 from the CC (CC2) had the lowest Pearson correlation coefficient (Figure S3). The particles used to acquire spectra in this sample were quite small (<50 μm) and interference from the filter may have added noise to the spectra. Also, insufficient material from the paint microplastics may have affected the signal intensity. Overall, comparing all the weathered paint microplastics to each other revealed high correlation coefficients. This confirms that the spectra, even among weathered paint microplastics, were very similar, with no substantial changes in the organic components of paint.

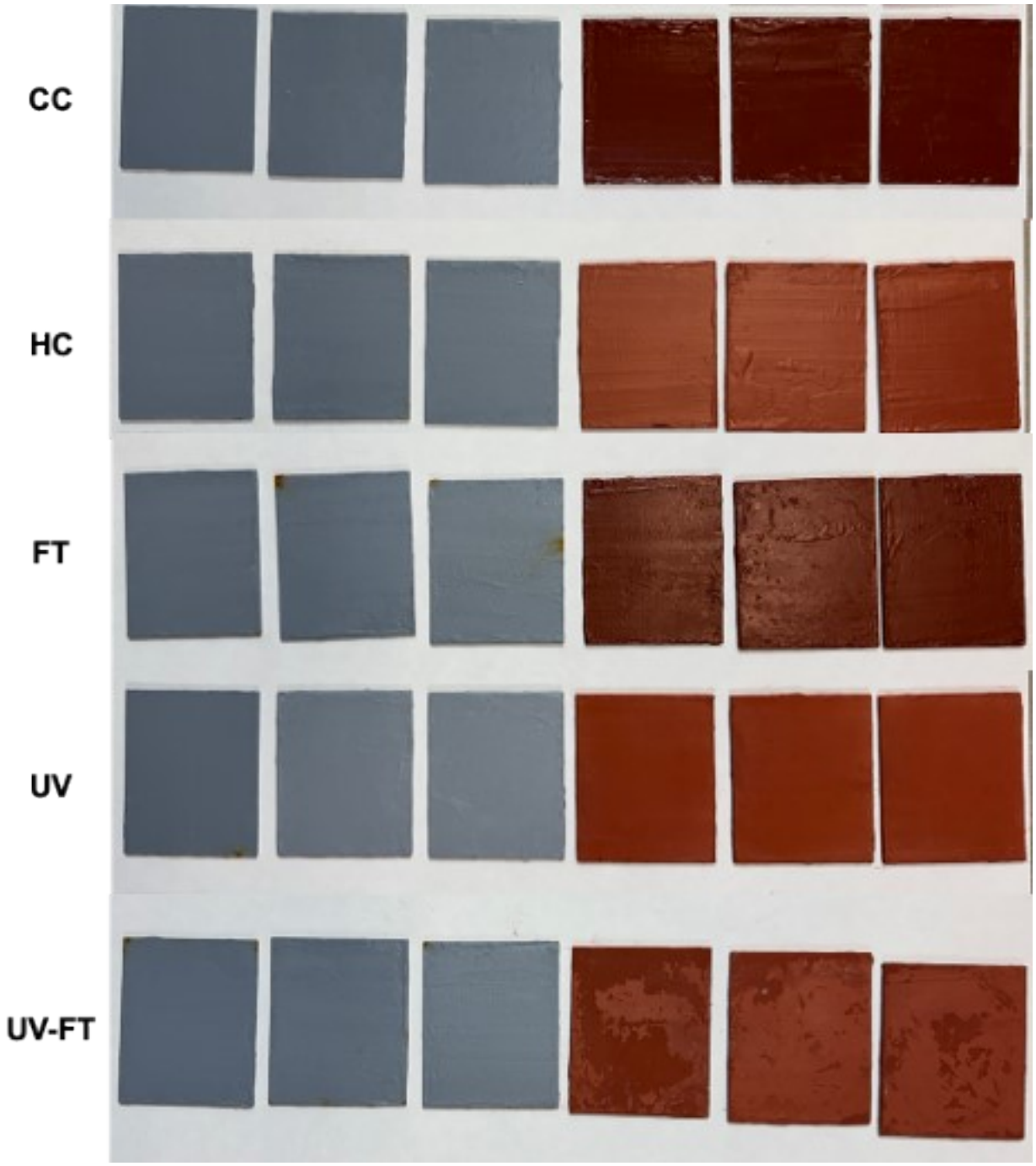

Figure S5. Representative images of coupons for primer paint (grey coupons) and antifouling paint (red coupons) after a six-week exposure to the different weathering treatments or controls. Treatments or controls are denoted as CC = cold control, HC = heat control, UV = UV irradiation, FT = freeze-thaw, and UV-FT = UV and FT combination.

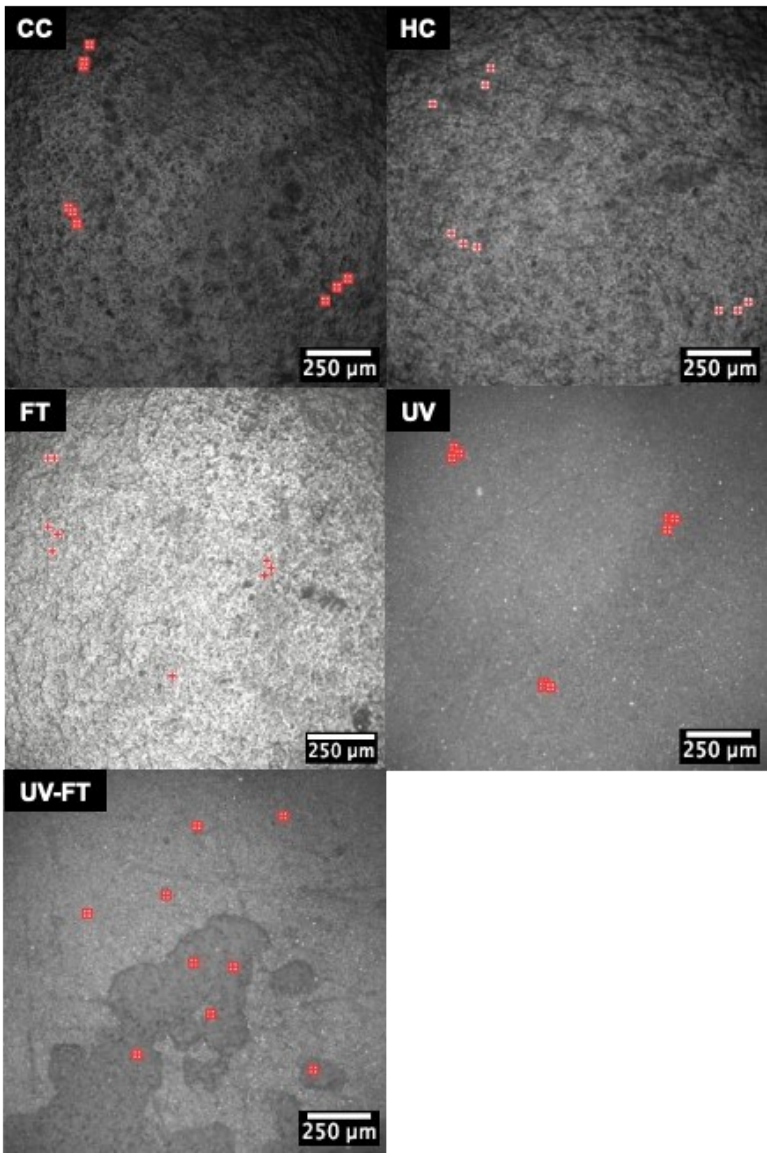

Figure S6. Representative images of coupons taken with the O-PTIR for antifouling paint after a six-week exposure to the different weathering treatment or controls. Treatments or controls are denoted as CC = cold control, HC = heat control, UV = UV irradiation, FT = freeze-thaw, and UV-FT = UV and FT combination. Red markers show spots where a spectrum was acquired.

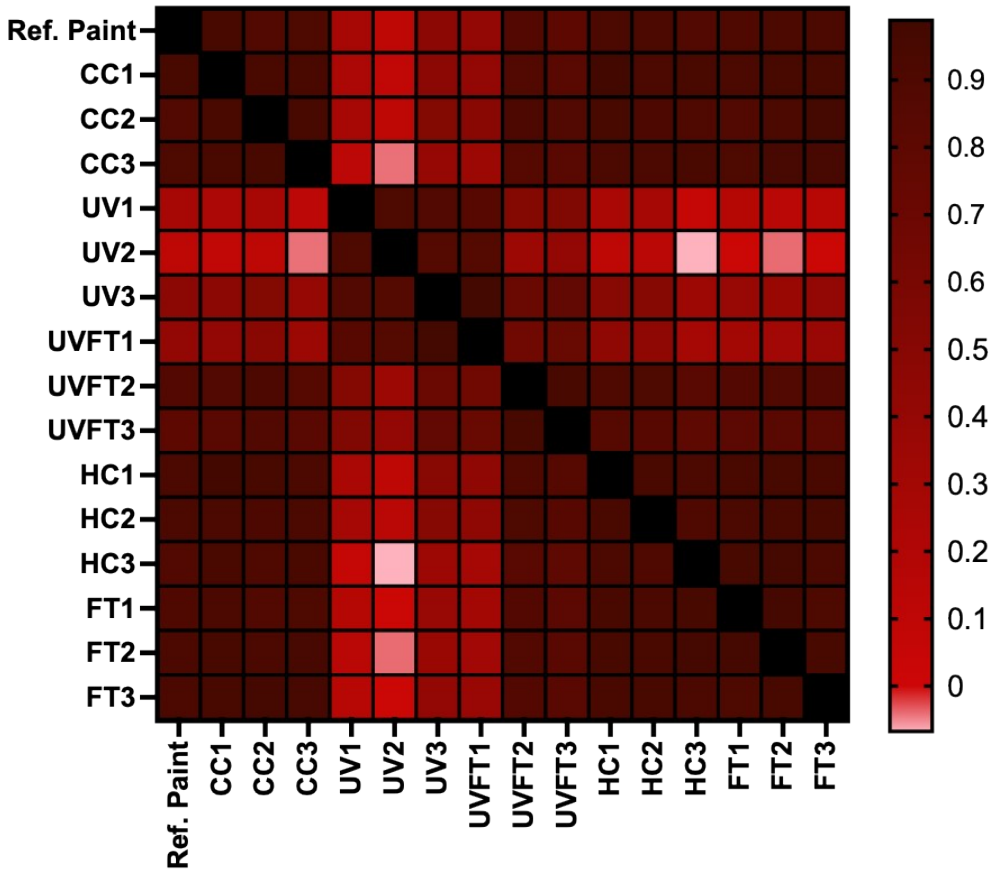

Figure S7. A heatmap of Pearson correlation coefficients comparing exposed antifouling paint coupons and reference antifouling paint (denoted as Ref. Paint). The average of nine spectra were used for each comparison. Treatments or controls are denoted as CC = cold control, HC = heat control, UV = UV irradiation, FT = freeze-thaw, and UV-FT = UV and FT combination. Each replicate is denoted after the treatment or control name. Black squares indicate the correlation is equal to 1.

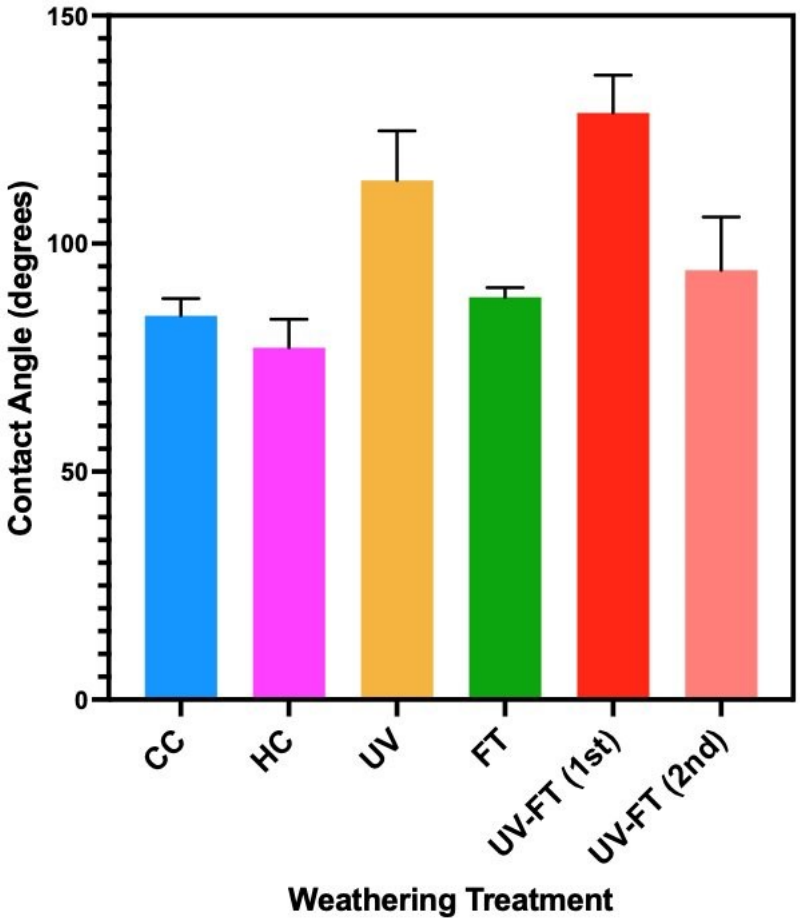

Figure S8. Contact angles (degrees) for water droplets on exposed antifouling paint coupons. Treatments or controls are denoted as CC = cold control, HC = heat control, UV = UV irradiation, FT = freeze-thaw, and UV-FT = UV and FT combination. The paint layer at which the contact angle for UV-FT was measured is indicated in parentheses. Error bars indicate standard deviation.

Table S3. Results of Mann-Whitney U-test comparing the water contact angles of the exposed antifouling paint coupons. Asterisks define significance, where: ns = nonsignificant, * = $p < 0.05$ significant, ** = $p < 0.01$ highly significant, and *** = $p < 0.001$ very highly significant.

Weathering treatment/control	Cold Control (CC)	Heat Control (HC)	Freeze-Thaw (FT)	UV	UV-FT (1st layer)	UV-FT (2nd layer)
Cold Control (CC)		*	ns	**	**	ns
Heat Control (HC)	*		*	**	**	*
Freeze-Thaw (FT)	ns	*		**	**	ns
UV	**	**	**		ns	*
UV-FT (1st layer)	**	**	**	ns		**
UV-FT (2nd layer)	ns	*	ns	*	**	

Table S4. Average Pearson correlation coefficient (n = 9) of weathered antifouling paint microplastics compared to weathered antifouling paint coupons.

Weathering treatment/control	*CC coupon*	*UV coupon*	*UV-FT coupon*	*HC coupon*	*FT coupon*
CC paint microplastics	**0.67**	0.35	0.62	0.69	0.69
UV paint microplastics	0.82	**0.43**	0.74	0.81	0.80
UV-FT paint microplastics	0.82	0.35	**0.72**	0.84	0.84
HC paint microplastics	0.73	0.31	0.65	**0.79**	0.80
FT paint microplastics	0.83	0.13	0.59	0.85	**0.87**

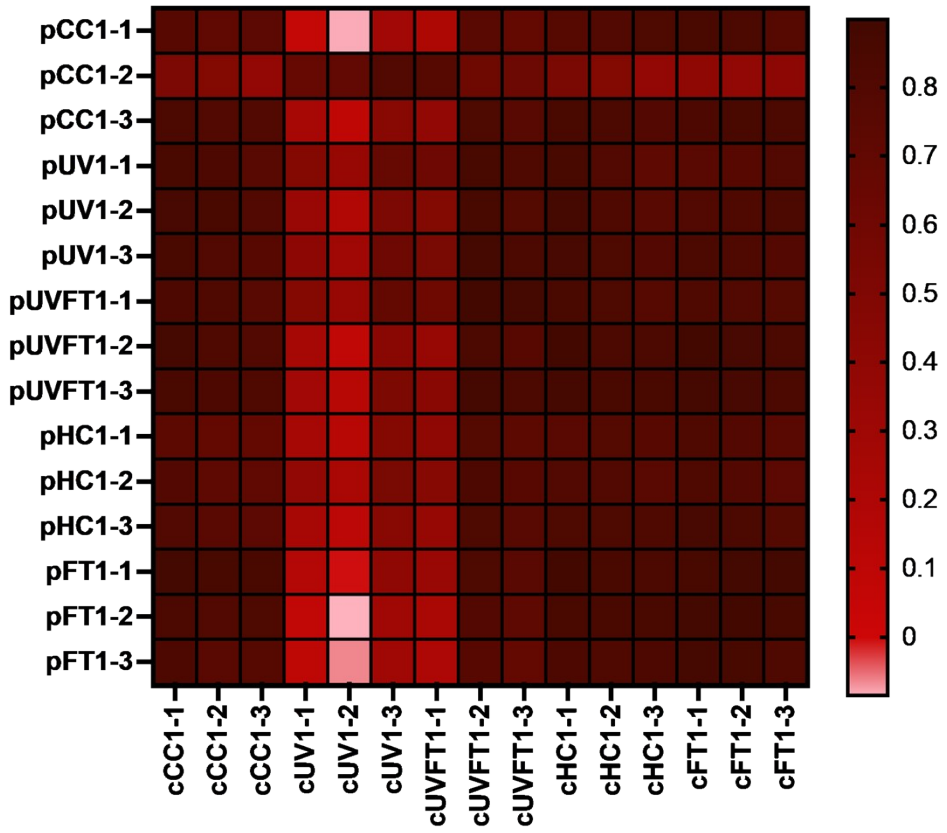

Figure S9. A heatmap of Pearson correlation coefficients comparing weathered antifouling paint microplastics and exposed antifouling paint coupons. The average of nine spectra were used for each comparison. Each comparison is denoted as either p = paint microplastics and c = coupon. Treatments or controls are denoted as CC = cold control, HC = heat control, UV = UV irradiation, FT = freeze-thaw, and UV-FT = UV and FT combination. Each replicate is denoted after the treatment or control name.

Table S5. Descriptive statistics of particle sizes and particle counts of microscopic images from weathered antifouling paint treatments and controls, analyzed using ImageJ. All values were blank subtracted.

Weathering treatment/control	Average median size (mm ± SD)	Average mean size (mm ± SD)	Average minimum size (mm ± SD)	Average maximum size (mm ± SD)	Average particle count (particles/mL ± SD)
Cold Control (CC)	0.03 ± 0.01	0.04 ± 0.007	0.007 ± 0.0002	0.7 ± 0.5	2 ± 3
Hot Control (HC)	0.02 ± 0.00	0.04 ± 0.02	0.007 ± 0.0002	1.1 ± 0.7	6 ± 6
Freeze-Thaw (FT)	0.03 ± 0.01	0.07 ± 0.02	0.006 ± 1E-18	3.3 ± 1.0	67 ± 30
UV	0.02 ± 0.00	0.03 ± 0.004	0.006 ± 0.0006	1.0 ± 0.3	14 ± 10
UV-FT*	N.D.	N.D.	N.D.	N.D.	N.D.

*Particle counts and size for UV-FT are not defined (N.D.) as the filter was saturated with particles.

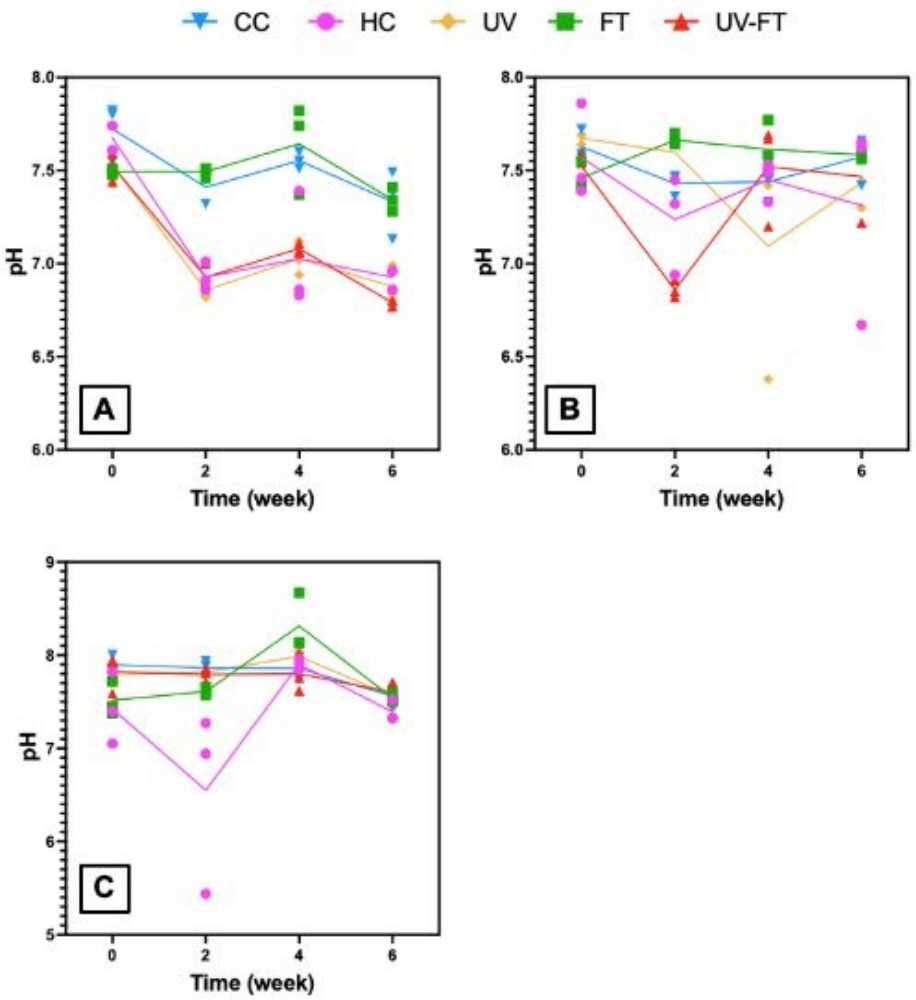

Figure S10. pH measurements for (A) antifouling paint, (B) primer paint and (C) procedural blanks exposed to the appropriate weathering treatment or control. The connected lines at each timepoint represent the median. Each replicate measurement is shown for every timepoint (n = 3).

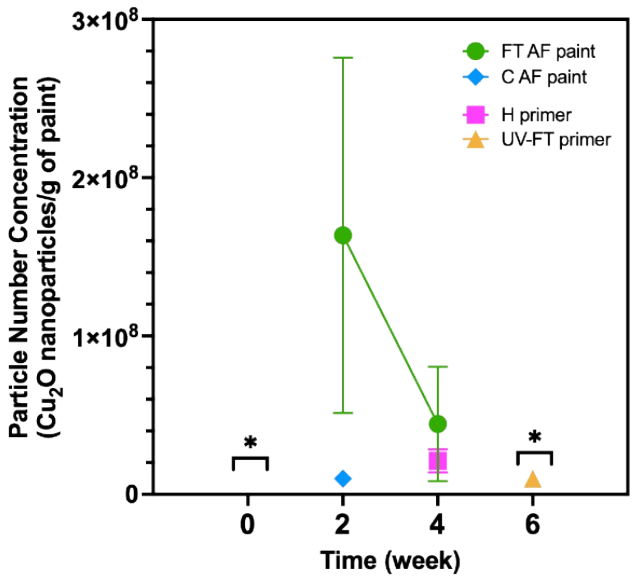

Figure S11. Average number concentrations of Cu_2O nanoparticles per gram of dry paint (number of nanoparticles/g of dry paint). Concentrations are shown for antifouling paints exposed to FT and CC treatments, and primer exposed to UV-FT and HC treatments as a function of time. Error bars denote standard deviation of triplicate measurements (n = 3). Asterisks denote time points that were statistically insignificant (i.e., <200 particle events).

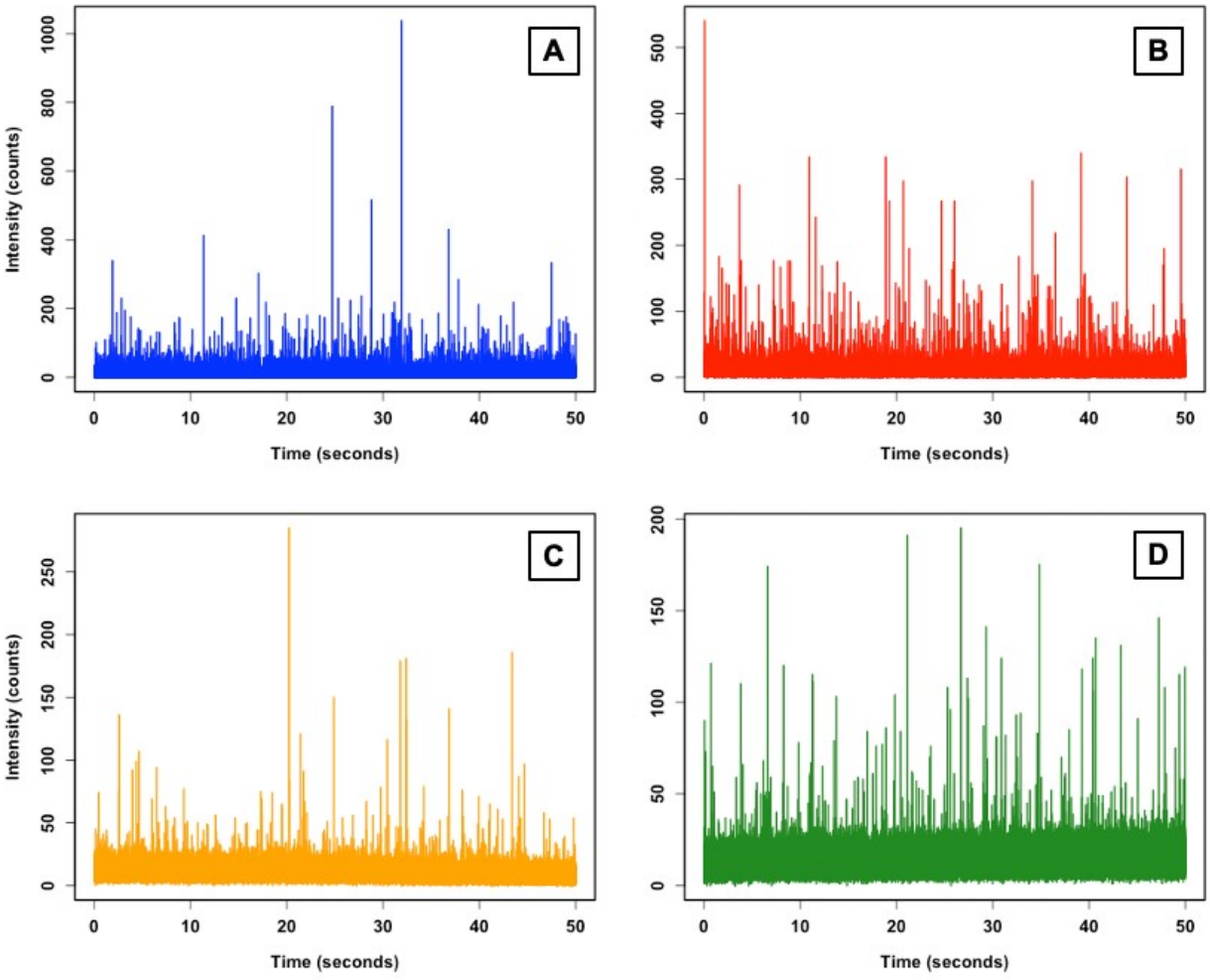

Figure S12. Representative examples of raw SP-ICP-MS data for Cu_2O released from antifouling paints exposed to (A) FT treatment at 2 weeks, (B) FT treatment at 4 weeks, (C) FT treatment at 6 weeks, and (D) CC control at 2 weeks.

Table S6. Average mass concentration (µg/L ± SD), average dissolved (ionic) background (µg/L ± SD), and fraction of average mass concentration of Cu_2O divided by the average dissolved background (% ± SD) obtained from untreated SP-ICP-MS data. Individual triplicates are shown for controls and weathering treatments.

Weathering treatment/control	Week	Average mass concentration (µg/L ± SD)	Average dissolved background (µg/L ± SD)	Average mass concentration divided by average dissolved background (% ± SD)
Cold Control (CC)	2	0.75 ± 0.2	17 ± 10	4.3 ± 6
		1.0 ± 1	11 ± 7	18 ±27
		1.2 ± 0.7	19 ± 11	6.4 ± 3
Freeze-Thaw (FT)	2	0.55 ± 0.06	3.6 ± 0.8	15 ± 1
		0.14 ± 0.01	2.0 ± 0.5	6.8 ± 1
		0.33 ± 0.05	3.2 ± 0.7	10 ± 1
	4	0.21 ± 0.06	4.1 ± 1	5.3 ± 2
		0.055 ± 0.004	2.4 ± 0.6	2.3 ± 0.4
		0.044 ± 0.004	3.2 ± 0.7	1.4 ± 0.36
	6	0.029 ± 0.004	3.8 ± 0.6	0.78 ± 0.09
		0.033 ± 0.008	6.2 ± 0.9	0.54 ± 0.07
		0.027 ± 0.003	7.7 ± 1	0.36 ± 0.09

References

1 A.-K. Müller, J. Brehm, M. Völkl, V. Jérôme, C. Laforsch, R. Freitag and A. Greiner, Disentangling biological effects of primary nanoplastics from dispersion paints' additional compounds, *Ecotoxicol. Environ. Saf.*, 2022, **242**, 113877.

2 C. Fang, W. Zhou, J. Hu, C. Wu, J. Niu and R. Naidu, Paint has the potential to release microplastics, nanoplastics, inorganic nanoparticles, and hybrid materials, *Environ. Sci. Eur.*, 2024, **36**, 17.

3 A. A. Horton, C. Svendsen, R. J. Williams, D. J. Spurgeon and E. Lahive, Large microplastic particles in sediments of tributaries of the River Thames, UK – Abundance, sources and methods for effective quantification, *Mar. Pollut. Bull.*, 2017, **114**, 218–226.

4 Y. K. Song, S. H. Hong, M. Jang, J.-H. Kang, O. Y. Kwon, G. M. Han and W. J. Shim, Large Accumulation of Micro-sized Synthetic Polymer Particles in the Sea Surface Microlayer, *Environ. Sci. Technol.*, 2014, **48**, 9014–9021.

5 A. L. d. F. Lacerda, L. dos S. Rodrigues, E. van Sebille, F. L. Rodrigues, L. Ribeiro, E. R. Secchi, F. Kessler and M. C. Proietti, Plastics in sea surface waters around the Antarctic Peninsula, *Sci. Rep.*, 2019, **9**, 3977.

6 M. M. Borges Ramirez, R. Dzul Caamal and J. Rendón von Osten, Occurrence and seasonal distribution of microplastics and phthalates in sediments from the urban channel of the Ria and coast of Campeche, Mexico, *Science of The Total Environment*, 2019, **672**, 97–105.

7 A. Turner, C. Ostle and M. Wootton, Occurrence and chemical characteristics of microplastic paint flakes in the North Atlantic Ocean, *Science of the Total Environment*, 2022, **806**, 150375.

8 M. F. Mengatto and R. H. Nagai, A first assessment of microplastic abundance in sandy beach sediments of the Paranaguá Estuarine Complex, South Brazil (RAMSAR site), *Mar. Pollut. Bull.*, 2022, **177**, 113530.

9 T. Mani, S. Primpke, C. Lorenz, G. Gerdts and P. Burkhardt-Holm, Microplastic Pollution in Benthic Midstream Sediments of the Rhine River, *Environ. Sci. Technol.*, 2019, **53**, 6053–6062.

10 C. Higgins and A. Turner, Microplastics in surface coastal waters around Plymouth, UK, and the contribution of boating and shipping activities, *Science of The Total Environment*, 2023, **893**, 164695.

11 D.-H. Chae, I.-S. Kim, S.-K. Kim, Y. K. Song and W. J. Shim, Abundance and Distribution Characteristics of Microplastics in Surface Seawaters of the Incheon/Kyeonggi Coastal Region, *Arch. Environ. Contam. Toxicol.*, 2015, **69**, 269–278.

12 O. Y. Kwon, J.-H. Kang, S. H. Hong and W. J. Shim, Spatial distribution of microplastic in the surface waters along the coast of Korea, *Mar. Pollut. Bull.*, 2020, **155**, 110729.

13 R. Jaouani, C. Mouneyrac, A. Châtel, F. Amiard, M. Dellali, H. Beyrem, A. Michelet and F. Lagarde, Seasonal and spatial distribution of microplastics in sediments by FTIR imaging throughout a continuum lake - lagoon- beach from the Tunisian coast, *Science of The Total Environment*, 2022, **838**, 156519.

14 J. A. Ivar do Sul, M. F. Costa and G. Fillmann, Microplastics in the pelagic environment around oceanic islands of the Western Tropical Atlantic Ocean, *Water Air Soil Pollut.*, 2014, **225**, 2004.

15 J.-H. Kang, O. Y. Kwon, K.-W. Lee, Y. K. Song and W. J. Shim, Marine neustonic microplastics around the southeastern coast of Korea, *Mar. Pollut. Bull.*, 2015, **96**, 304–312.
16 A. R. A. Lima, M. F. Costa and M. Barletta, Distribution patterns of microplastics within the plankton of a tropical estuary, *Environ. Res.*, 2014, **132**, 146–155.
17 H. K. Imhof, C. Laforsch, A. C. Wiesheu, J. Schmid, P. M. Anger, R. Niessner and N. P. Ivleva, Pigments and plastic in limnetic ecosystems: A qualitative and quantitative study on microparticles of different size classes, *Water Res.*, 2016, **98**, 64–74.
18 C. Leistenschneider, P. Burkhardt-Holm, T. Mani, S. Primpke, H. Taubner and G. Gerdts, Microplastics in the Weddell Sea (Antarctica): A Forensic Approach for Discrimination between Environmental and Vessel-Induced Microplastics, *Environ. Sci. Technol.*, 2021, **55**, 15900–15911.
19 C. Dibke, M. Fischer and B. M. Scholz-Böttcher, Microplastic Mass Concentrations and Distribution in German Bight Waters by Pyrolysis–Gas Chromatography–Mass Spectrometry/Thermochemolysis Reveal Potential Impact of Marine Coatings: Do Ships Leave Skid Marks?, *Environ. Sci. Technol.*, 2021, **55**, 2285–2295.
20 A. Gondikas, K. Mattsson and M. Hassellöv, Methods for the detection and characterization of boat paint microplastics in the marine environment, *Frontiers in Environmental Chemistry*, DOI:10.3389/fenvc.2023.1090704.
21 S. Zuin, M. Gaiani, A. Ferrari and L. Golanski, Leaching of nanoparticles from experimental water-borne paints under laboratory test conditions, *Journal of Nanoparticle Research*, 2014, **16**, 2185.
22 A. Al-Kattan, A. Wichser, R. Vonbank, S. Brunner, A. Ulrich, S. Zuin, Y. Arroyo, L. Golanski and B. Nowack, Characterization of materials released into water from paint containing nano-SiO2, *Chemosphere*, 2015, **119**, 1314–1321.
23 X. Zhang, M. Wang, S. Guo, Z. Zhang and H. Li, Effects of weathering and rainfall conditions on the release of SiO2, Ag, and TiO2 engineered nanoparticles from paints, *Journal of Nanoparticle Research*, 2017, **19**, 338.
24 A. Azimzada, J. M. Farner, M. Hadioui, C. Liu-Kang, I. Jreije, N. Tufenkji and K. J. Wilkinson, Release of TiO 2 nanoparticles from painted surfaces in cold climates: characterization using a high sensitivity single-particle ICP-MS, *Environ. Sci. Nano*, 2020, **7**, 139–148.
25 R. Kaegi, A. Ulrich, B. Sinnet, R. Vonbank, A. Wichser, S. Zuleeg, H. Simmler, S. Brunner, H. Vonmont, M. Burkhardt and M. Boller, Synthetic TiO2 nanoparticle emission from exterior facades into the aquatic environment, *Environmental Pollution*, 2008, **156**, 233–239.
26 I. Jreije, A. Azimzada, M. Hadioui and K. J. Wilkinson, Stability of CeO 2 nanoparticles from paints and stains: insights under controlled and environmental scenarios, *Environ. Sci. Nano*, 2022, **9**, 3361–3371.
27 R. Kaegi, B. Sinnet, S. Zuleeg, H. Hagendorfer, E. Mueller, R. Vonbank, M. Boller and M. Burkhardt, Release of silver nanoparticles from outdoor facades, *Environmental Pollution*, 2010, **158**, 2900–2905.
28 A. S. Adeleye, E. A. Oranu, M. Tao and A. A. Keller, Release and detection of nanosized copper from a commercial antifouling paint, *Water Res.*, 2016, **102**, 374–382.
29 A. Azimzada, J. M. Farner, I. Jreije, M. Hadioui, C. Liu-Kang, N. Tufenkji, P. Shaw and K. J. Wilkinson, Single- and Multi-Element Quantification and Characterization of TiO2

Nanoparticles Released From Outdoor Stains and Paints, *Front. Environ. Sci.*, DOI:10.3389/fenvs.2020.00091.

30 A. Al-Kattan, A. Wichser, R. Vonbank, S. Brunner, A. Ulrich, S. Zuin and B. Nowack, Release of TiO2 from paints containing pigment-TiO2 or nano-TiO2 by weathering, *Environ. Sci. Process. Impacts*, 2013, **15**, 2186.

31 N. Singh and A. Turner, Trace metals in antifouling paint particles and their heterogeneous contamination of coastal sediments, *Mar. Pollut. Bull.*, 2009, **58**, 559–564.

32 A. Jalaie, A. Afshaar, S. B. Mousavi and M. Heidari, Investigation of the Release Rate of Biocide and Corrosion Resistance of Vinyl-, Acrylic-, and Epoxy-Based Antifouling Paints on Steel in Marine Infrastructures, *Polymers (Basel).*, 2023, **15**, 3948.

33 M. Simon, A. Vianello, Y. Shashoua and J. Vollertsen, Accelerated weathering affects the chemical and physical properties of marine antifouling paint microplastics and their identification by ATR-FTIR spectroscopy, *Chemosphere*, 2021, **274**, 129749.

34 L. Holmes and A. Turner, Leaching of hydrophobic Cu and Zn from discarded marine antifouling paint residues: Evidence for transchelation of metal pyrithiones, *Environmental Pollution*, 2009, **157**, 3440–3444.

35 A. Jessop and A. Turner, Leaching of Cu and Zn from discarded boat paint particles into tap water and rain water, *Chemosphere*, 2011, **83**, 1575–1580.

36 Interlux, *Micron CSC - CA Red - Safety Datasheet*, 2021.

37 Interlux, *Interprotect Grey Base - Safety Datasheet*, 2014.

38 Chemical Book, Rosin(8050-09-7) IR2, https://www.chemicalbook.com/SpectrumEN_8050-09-7_IR2.htm, (accessed 29 January 2026).